Electronic Supplementary Information

Substrate coating by conductive polymers through spontaneous oxidation and polymerization

Kento Kuwabara, Hirotaka Masaki, Hiroaki Imai, Yuya Oaki*

Department of Applied Chemistry, Faculty of Science and Technology, Keio University, 3-14-1 Hiyoshi, Kohoku-ku, Yokohama 223-8522, Japan.

E-mail: oakiyuya@applc.keio.ac.jp

Contents

Experimental methods

Syntheses of the heteroaromatic polymers. All the reagents were used as purchased without further purification. The following substrates were used for the coating: glass, alkyl-modified glass, polytetrafluoroethylene (PTFE), indium tin oxide (ITO), graphite, and metallic titanium mesh. The following heteroaromatic monomers were used: pyrrole (Py, Kanto, 99.0%), 1-methylpyrrole (Py-1Me, TCI, 99.0%), 3-methylpyrrole (Py-3Me, TCI, 98.0%), thiophene (Tp, TCI, 98.0%), 3,4-ethylenedioxythiophene (EDOT, TCI, 98.0%), 3-methoxythiophene (Tp-OMe, Wako, 98.0%), and 3-hexylthiophene (3HT, TCI, 98.0 %)). The typical experimental setup was shown in Fig. 1b. Neat liquid of the heteroaromatic monomers, typically 0.05 cm^3, was poured in a glass bottle 40 cm^3 in volume. A small vessel containing 0.1 mg of $Fe(NO_3)_3 \cdot 9H_2O$ (Kanto, 99.0 %) was set in the center of the glass bottle. The substrates were attached on the cover of the outer glass bottle by using a tape. When carbon black (CB) and purified water were used as the substances, the smaller sample bottle containing the powder and the liquid was set in the glass bottle. After the sealing, the sample bottle was maintained at 60 °C for the certain period. The resultant coating on the substrates was washed with acetone and then dried.

Characterization. The morphology of the coating was observed by field-emission scanning electron microscopy (FESEM, FEI Sirion, Hitachi S-4700, and JEOL JSM 7800F). The PPy thin coating on CB nanoparticles was analyzed by FESEM (Carl Zeiss, MERLIN VP compact) with BSE detector and EDX equipment (Bruker, Quantax) operated at 1.2–2.0 kV. The structure characterization was performed by Fourier-transfer infrared absorption spectroscopy (FT-IR, Jasco FT/IR 4200). The coating on the substrates was directly analyzed by attenuated total reflection (ATR) method. When the coating was removed from the substrate, the powdered sample was measured by KBr method. The specific surface area was calculated by the BET method using nitrogen adsorption isotherms obtained at 77 K (Micromeritics, 3Flex).

Physicochemical properties of the monomers. The oxidation potential of the monomers was measured by using a three electrode setup in a beaker cell. ITO substrate, platinum wire, and $Ag/AgNO_3$ were used as the working, counter, and reference electrodes, respectively. The electrolyte solution was the acetonitrile solution containing 0.1 mol dm^{-3} of tetrabutylammonium perchlorate. Linear sweep voltammetry (LSV) measurement was performed by using potentiostat (Hokuto Denko, HSV-100) in the potential range from 0.5 V

to 2.9 V vs. $Ag/AgNO_3$ at 100 mV s^{-1}. The redox potential in the acetonitrile solution was calibrated by that of ferrocene and ferrocenium (Fc/Fc^+). The contact angle of the Py monomer liquid on substrates in Table 2 was measured by using a contact angle meter (Kyowa Interface, DMe-201).

Electrochemical properties of the PPy coated CB nanoparticles. The CB nanoparticles was mixed with poly(vinylidene fluoride) (PVDF) as a binder in *N*-methylpyrrolidone by the weight ratio of 9/1. The mixture of the CB and PVDF was pasted on Ti mesh. Then, the PPy coating was performed in the reaction chamber as shown in Fig. 1b. The PPy-coated titanium mesh was directly used as the working electrode. The measured weight of the related materials was summarized in Tables S2 and S3. A platinum wire and Ag/AgCl electrode were used as the counter and reference electrodes, respectively. The electrolyte was 1 mol dm^{-3} sulfonic acid (H_2SO_4) aqueous solution. Cyclic voltammetry was measured by using potentiostat (Princeton Applied Research, VersaSTAT 3) in the potential range from 0 V to 0.8 V vs. Ag/AgCl at 500, 1000, 2000, and 5000 mV s^{-1}.

FT-IR spectra of the heteroaromatic polymers coated on substrates

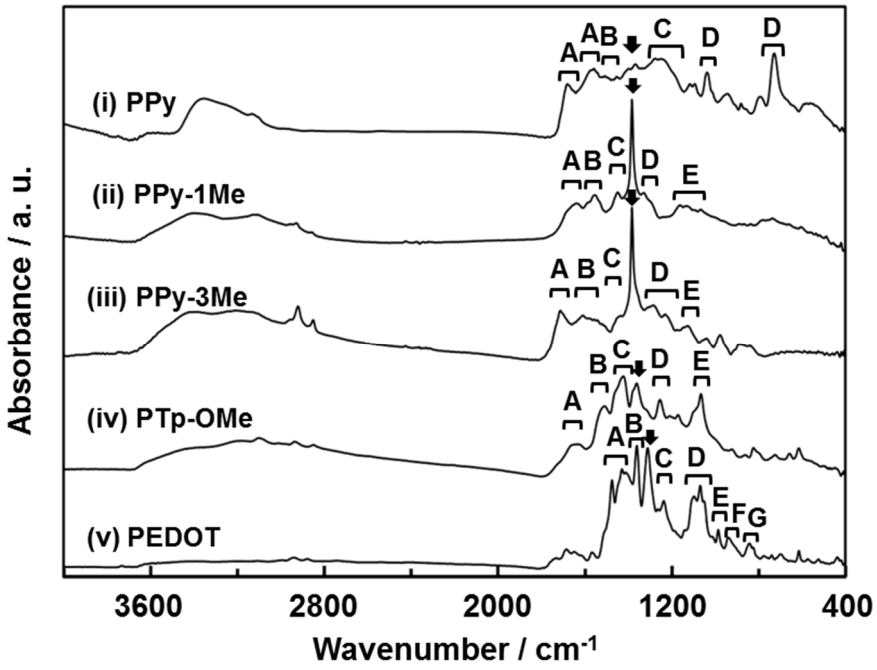

Fig. S1. FT-IR spectra of the PPy coating for 60 h (i), the PPy-1Me coating for 0.5 h (ii), the PPy-3Me coating for 7 h (iii), the PTp-OMe coating for 60 h (iv), and PEDOT coating for 60 h (v). The coating time was controlled to obtain an appropriate amount of the sample for the FT-IR analysis.

The absorption bands A–E in each spectrum were assigned to the following vibrations characteristic to PPy (i),[S1] PPy-1Me (ii), [S2] PPy-3Me (iii), [S3] PTp-OMe (iv), [S4] and PEDOT (v) [S5]: (i) C=C stretching (A), C–N stretching (B), C–C and C–H stretching (C), C–H out-of-plane bending (D). (ii) C=O stretching (A), C=C stretching (B), C–N stretching (C), C–H in-plane bending (D), C–H out-of-plane bending (E). (iii) C=O stretching (A), C=C stretching (B), C–N stretching (C), C–H in-plane bending (D), C–H out-of-plane bending (E). (iv) C–S stretching (A), C=C stretching (B), C–H in-plane bending (C), C–O–C stretching (D), and C–O stretching (E). (v) C=C stretching (A), C–H stretching (B), unknown but characteristic (C), C–O stretching (D), C–N stretching (E), C–S stretching (F), C–C–O stretching (G). These characteristic absorptions and the broadening of the bands suggest the formation of the heteroaromatic polymers.

The absorption bands with the black arrow is assigned to the N–O stretching vibration of

the nitro group introduced in the heteroaromatic rings. The results suggest that the activated monomers in the present system.

Additional references

S1. (a) R. Costić, D. Raković, S. A. Stepanyan, I. E. Davidova, L. A. Gribov, *J. Chem. Phys.* **1995**, *102*, 3104. (b) K. Majid, R. Tabassum, A. F. Shah, S. Ahmad, M. L. Singla, *J. Mater. Sci. Mater. Electron* **2009**, *20*, 958.

S2. M. I. Redondo, E. Sánchez de la Blanca, M. V. García, M. A. Raso, J. Tortajada, M. J. González-Tejera, *Synth. Met.* **2001**, *122*, 431.

S3. E. Sánchez de la Blanca, I. Carrillo, M. I. Redondo, M. J. González-Tejera, M. V. García, *Thin Solid Films* **2007**, *515*, 5248.

S4.(a) S. Tanaka, K. Kaeriyama, *Bull. Chem. Soc. Jpn.* **1989**, *62*, 1908. (b) Z. Han, J. Zhang, X. Yang, H. Zhu, W. Cao, *Solar Energy Mater. Solar Cells*. **2010**, *94*, 755.

S5. F. Tran-Van, S. Garreau, G. Louarn, G. Froyer, C. Chevrot, *J. Mater. Chem.* **2001**, *11*, 1378.

Time-course cross-sectional SEM images of the coating

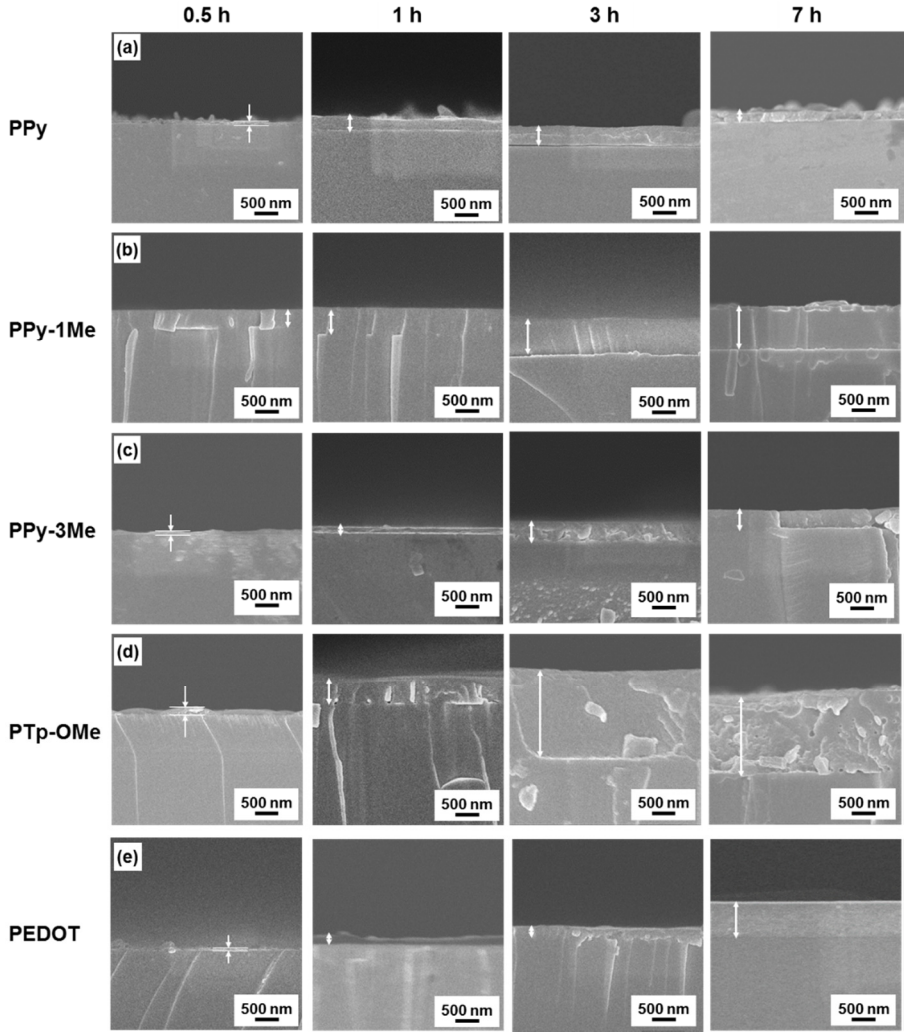

Fig. S2. Cross-sectional FESEM images of the PPy (a), PPy-1Me (b), PPy-3Me (c), PTp-OMe (d), and PEDOT (e) coating on glass substrate for 0.5 h, 1 h, 3 h, and 7 h.

The PPy-coated substrate was cut after scratching on the backside. As shown in the white arrows, the thickness on the substrate was measured. Based on these data, Fig. 2c summarizes the relationship between the coating time and thickness.

Oxidation potential of the heteroaromatic monomers

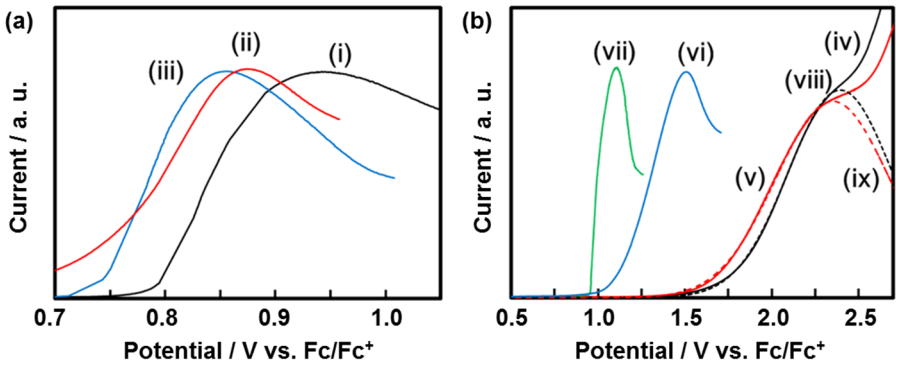

Fig. S3. LSV curves of the Py (a) and Tp derivatives (b). (a) LSV curves of Py (i), Py-3Me (ii), and Py-1Me (iii). (b) LSV curves of Tp (iv), 3HT (v), Tp-OMe (vi), EDOT (vii). The curves (iv) and (v) were respectively separated to the peaks (viii) and (ix) because the second oxidation peak was overlapped.

The peak top was defined as the oxidation potential of these monomers (Table 1).

SEM images of the PPy coating on ITO substrate

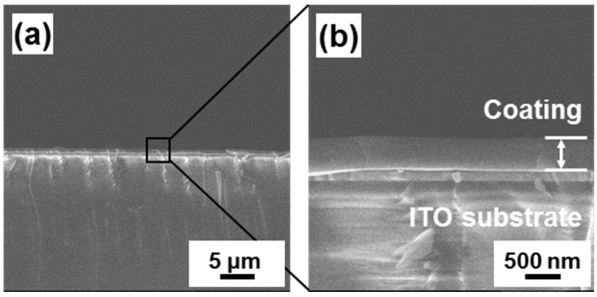

Fig. S4. SEM images of the PPy coating on ITO substrates for 2 h.

The flat thin-coating was obtained on ITO substrate, as well as glass substrate.

BET surface area of the CB nanoparticles

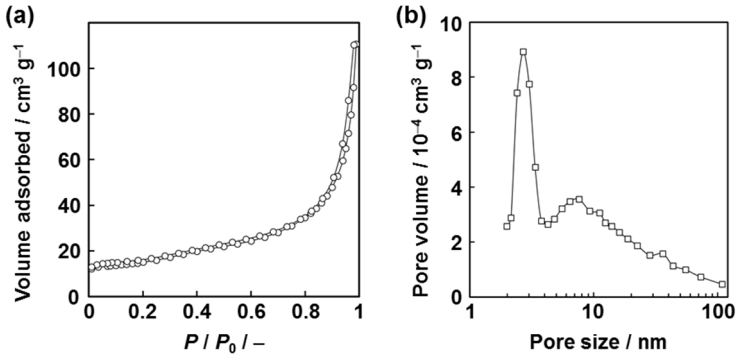

Fig. S5. Nitrogen adsorption-desorption isotherm (a) and pore-size distribution (b) of the CB nanoparticles.

The BET surface area was estimated to be 51.8 $m^2 g^{-1}$.

Calculation procedure of the specific capacity

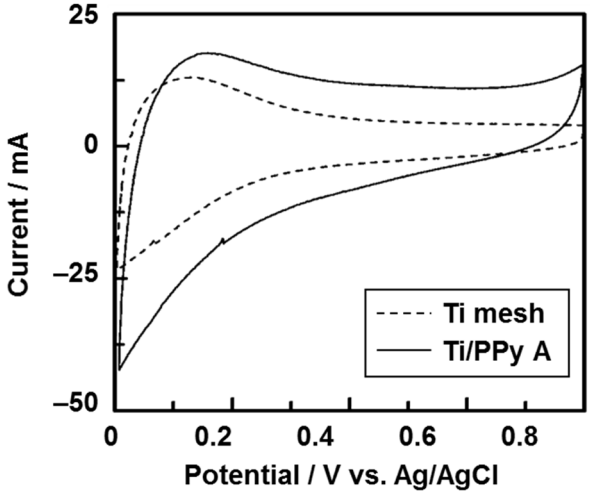

Fig. S6. CV curve of the Ti/PPy-A sample (the solid line) and the Ti mesh before the coating (the dashed line).

The specific capacity of the PPy thin layer was estimated from the CV curve with subtraction of the contribution from the substrates, such as CB nanoparticles on Ti mesh for CB/PPy samples (Fig. 5) and Ti mesh for Ti/PPy samples (Fig. S6). Here, the Ti/PPy-A sample was used as the model for explanation of the calculation method. The charge of the Ti/PPy (Q_1) and Ti (Q_2) was calculated from the CV curves. The difference ($\Delta Q = Q_1 - Q_2$) is the charge originating from the coated PPy (eq. S1).

$$\Delta Q = Q_1 - Q_2 = 0.0198 - 00105 = 0.0093 \text{ C} \ldots \text{(eq. S1)}$$

The specific capacity of the coated PPy is calculated by the (eq. S2), where W_{PPy} is the coated amount of PPy and ΔV is the potential range.

$$C_{PPy} = \frac{\Delta Q}{W_{PPy} \cdot \Delta V} = \frac{0.0093}{109 \times 10^{-6} \times 0.8} = 107 \text{ F g}^{-1} \ldots \text{(eq. S2)}$$

The other data were calculated by the same procedure (Figs. 5c and S8e).

Reproducibility of the specific capacity of the CB/PPy samples

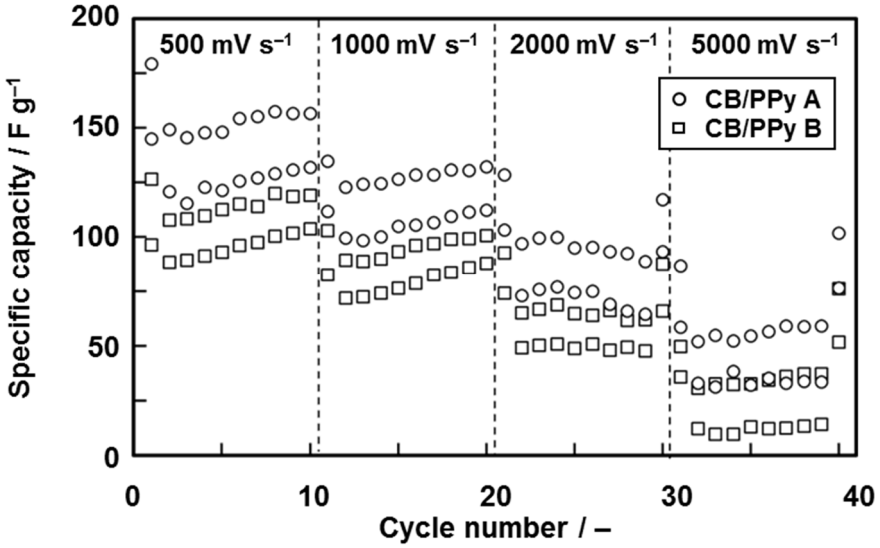

Fig. S7. Relationship between the scan rate and the specific capacity of the CB/PPy samples.

The same symbols represent the same samples. The data support the reproducibility of the electrochemical properties in the present work. The better data in Fig. S7 were used for preparation of Fig. 5c in the main text.

Direct PPy thin coating on a metallic Ti mesh

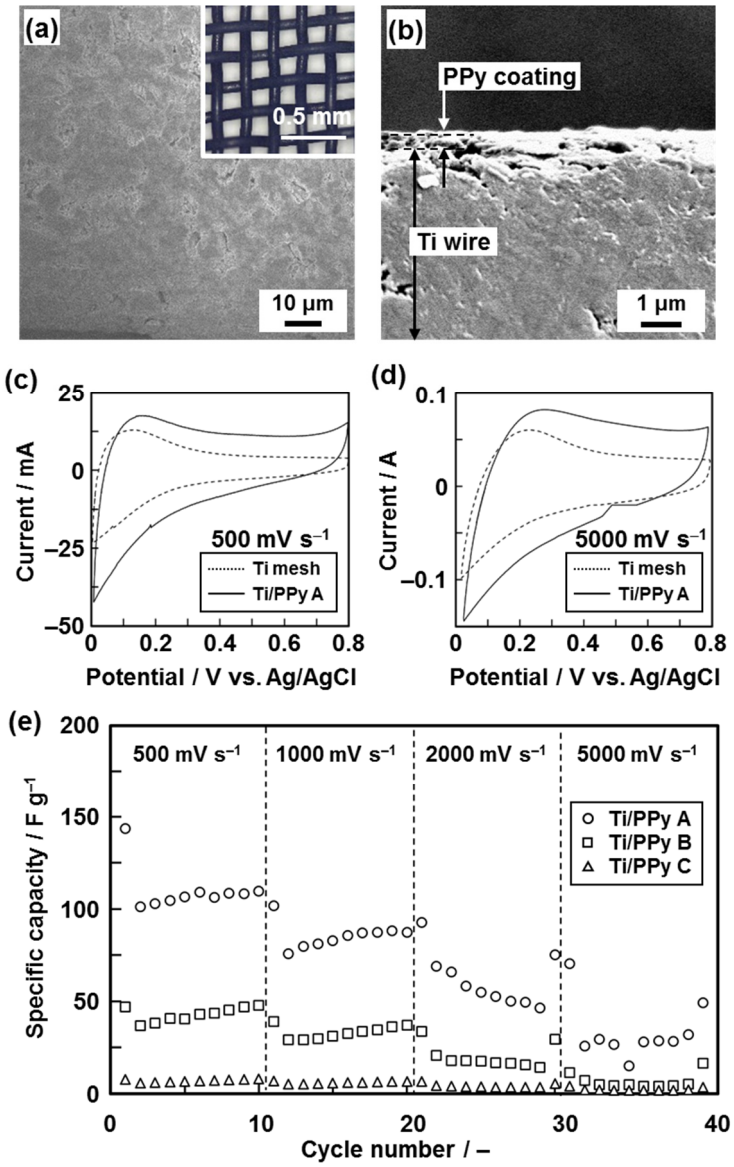

Fig. S8. Direct PPy coating on metallic Ti mesh. (a) Photograph (the inset) and the SEM image of the PPy-coated Ti mesh. (b) Cross-sectional SEM image of the PPy-coated Ti mesh. (c,d) CV curves of the Ti/PPy-A sample (the solid line) and the bare Ti mesh (the dashed line) at the scan rate of 500 mV sec^{-1} (c) and 5000 mV sec^{-1} (d). (e) Relationship between the scan rate and the specific capacity of the samples Ti/PPy A, B, and C with the different coating amount. The reproducibility of the specific capacity was described with Fig. S9.

In addition to the CB nanoparticles, the PPy thin coating was performed on Ti mesh as a current collector. A Ti mesh consisted of the wires around 100 μm (the inset of Fig. S8a). The PPy thin layers with the different coating amount were synthesized on a Ti mesh by changes of the

reaction time. The samples are classified into the three types depending on the weight ratio of the PPy (W_{PPy} / mg) to the Ti mesh (W_{Ti} / g), such as W_{PPy} / W_{Ti} = 0.5–0.8 mg g^{-1} for 0.5 h (Ti/PPy-A), W_{PPy} / W_{Ti} = 2.7–3.4 mg g^{-1} for 3 h (Ti/PPy-B), and W_{PPy} / W_{Ti} = 6.2–6.5 mg g^{-1} for 9 h (Ti/PPy-C) (Table S3). The flat coating around 100 nm in thickness was obtained on the surface of Ti mesh (Fig. S8a,b). The consecutive redox reaction characteristic to PPy was observed within 0–0.8 V vs. Ag/AgCl on the cyclic voltammograms (CV) at the high scan rate, such as 500 mV s^{-1} and 5000 mV s^{-1} (Fig. S8c,d). The CV measurement was performed on the metallic Ti mesh and the Ti/PPy samples (the dashed and solid lines in Fig. S8c,d). Since the weight ratio of the coated PPy was small, the capacity included the reaction of the Ti mesh. The specific capacity of the PPy thin layer was estimated from the CV curve with subtraction of the contribution from the metallic Ti mesh (Fig. S6). The Ti/PPy-A showed the specific capacity 106 F g^{-1} and 29.2 F g^{-1} at the high scan rate of 5000 mV s^{-1} and 5000 mV s^{-1}, respectively (Fig. S8c,d). Fig. S8e summarizes the specific capacity of all the samples at the different scan rates. The data of the specific capacity was reproducible (Fig. S9). The specific capacity was decreased with an increase in the weight of the PPy coating. The results indicate that the thinner PPy coating contributes to the higher specific capacity at the high scan rate. The thick coating of PPy is not fully used for the redox reaction at the high scan rate. Therefore, the CB/PPy with the thinner coating showed the enhanced high-rate performance (Fig. 5).

Reproducibility of the specific capacity of the Ti/PPy samples

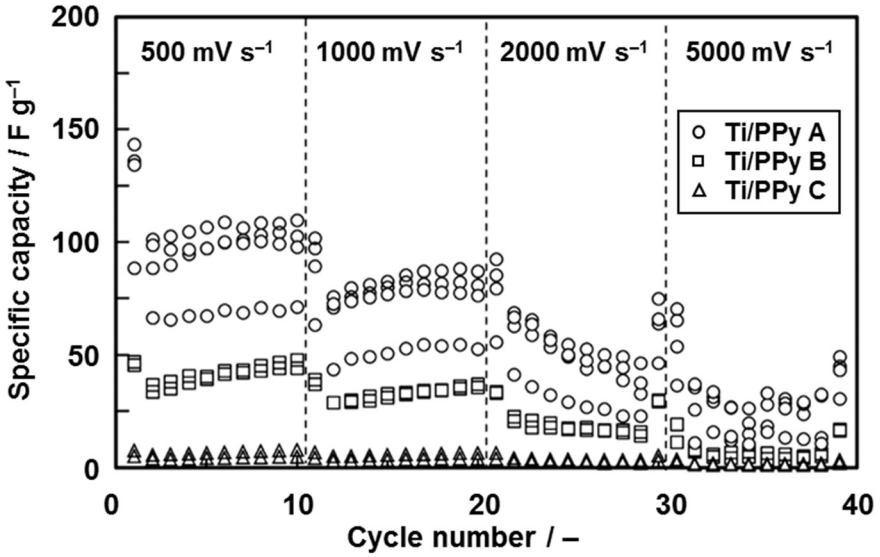

Fig. S9. Relationship between the scan rate and the specific capacity of the Ti/PPy samples.

The same symbols represent the same samples. The data support the reproducibility of the electrochemical properties in the present work. The better data in Fig. S9 were used for preparation of Fig. S8e.

Previous studies of the PPy coating on a current collector

Table S1. Previous reports about specific capacity of the PPy coating on a current collector at scan rate higher than 500 mV s^{-1}.

No.	Capacity / F g^{-1}	Scan rate / mV s^{-1}	Morphology (Synthetic approach)	Potential range / V	Electrolyte solution or electrode setup	Ref
1	280 265	500 1000	Film consisting of particle (Pulse electro-polymerization)	1.3	1 mol dm^{-3} KCl aq.	14*a*
2	250 205	500 2000	Film consisting of particle (Pulse electro-polymerization)	0.8	3 mol dm^{-3} KCl aq.	14*b*
3	200	500	Film consisting of particle (Pulse electro-polymerization)	1.6	1 mol dm^{-3} KCl aq.	14*c*
4	100	500	Film consisting of particle (Pulse electro-polymerization)	0.6	Solid electrode with a gel electrolyte	14*d*
5	130 120	500 1000	Flat thin film (Electro-polymerization)	1.2	Solid electrode with a gel electrolyte	14*e*

In previous reports,[14] PPy synthesized by electro-polymerization was used for the high-rate charge storage. The specific capacity and the related data are summarized in Table S1. The data measured on CV at the scan rate higher than 500 mV s^{-1} were only extracted.

Sample list of the PPy coating on the CB nanoparticles

Table S2. Sample list of the PPy-coated CB powder.

Group	No.	Weigh of Ti mesh W_{Ti} / mg	Weigh of CB and PVDF $W_{CB+PVDF}$ / μg	Weigh of CB W_{CB} / mg	Weigh of PPy-coated CB W_{CB-PPy} / mg	Weight of coated PPy W_{PPy} / μg	Weight ratio W_{PPy} / W_{CB} / g g^{-1}
CB/PPy-A	1	98.382	1216	99.598	99.89	292	0.300
	2	100.366	1452	101.818	102.114	296	0.255
CB/PPy-B	1	97.561	1589	99.15	99.565	415	0.326
	2	92.212	1241	93.453	93.876	423	0.426
CB/PPy-C	1	97.153	1414	98.567	99.049	482	0.426
	2	96.458	1345	97.803	98.415	612	0.569

The samples were categorized into three types depending on the weight of the coated PPy (g) to that of the CB (g), such as ca. 0.2–0.3 g g^{-1} for 1 h (CB/PPy-A), 0.3–0.4 g g^{-1} for 3 h (CB/PPy-B), and 0.4–0.6 g g^{-1} for 6 h (CB/PPy-C).

Sample list of the PPy coating on Ti mesh

Table S3. Sample list of the PPy-coated Ti mesh.

Group	No.	Weigh of Ti mesh	Weight of the PPy-coated Ti mesh	Weight of the PPy	Weight ratio
		W_{Ti} / mg	$W_{Ti\text{-}PPy}$ / mg	W_{PPy} / μg	W_{PPy} / W_{Ti} / mg g^{-1}
Ti/PPy-A	1	151.435	151.544	109	0.72
	2	152.469	152.566	97	0.64
	3	149.179	149.296	116	0.78
	4	150.006	150.086	80	0.53
Ti/PPy-B	1	148.600	149.103	503	3.38
	2	144.220	144.611	391	2.71
Ti/PPy-C	1	144.851	145.804	953	6.58
	2	147.360	148.280	920	6.24

The samples are classified into the three types depending on the weight ratio of the coated PPy (mg) to the Ti mesh (g), such as ca. 0.5–0.8 mg g^{-1} for 0.5 h (Ti/PPy-A), 2.7–3.4 mg g^{-1} for 3 h (Ti/PPy-B), and 6.2–6.5 mg g^{-1} for 6 h (Ti/PPy-C).